Journal of the Ghana Institution of Engineering (2023) 23:3
https//doi.org/10.56049/jghie.v23i3.100

CASE STUDY

Evaluation of porosity and permeability of sandstones within the Oti Group of the Volta Basin using petrophysical and petrographic techniques

Theresa N. Zobah[1], Caspar D. Adenutsi[2,*], Godfrey C. Amedjoe[1], Matthew C. Wilson[1], Emmanuel Mensah[1], Cyril D. Boateng[3], Kwame K. Sarpong[2], Lydia N. O. Opuni[1], Sylvester K. Danuor[3], Hassan Karimaie[2]

Received: 7th March, 2023 / **Accepted:** 19th August, 2023
Published online: 18th September, 2023

Abstract
This study investigates the reservoir quality of sandstones in the Oti Group of the Volta Basin of Ghana. Geological field mapping, petrographic, petrophysical, mineralogical, and geochemical techniques are used to investigate the reservoir parameters of the sandstones by evaluating the fluid holding and transmission capabilities of the rocks. Results from the comprehensive study identified two sandstone formations of interest; viz. the Bimbila Sandstone and Yabraso Sandstone. Both sandstones were found to be quartz sandstones (sub-arkose and quartz arenites). The Bimbila Sandstones proved to have better porosity and permeability as compared to the Yabraso Sandstones. The Yabraso Sandstone showed porosity between 7-22 % with an average porosity of 13 % (helium gas) and permeability of 63.41 mD, which may be linked to intense cementation and intermediate compaction as well as grain size, shape and arrangement. The Bimbila Sandstones showed better porosity and permeability with a porosity range of 6-24 %, an average porosity of 14 % (helium gas) and 131.80 mD permeability. This is seen to be due to lower compaction supported by framework-stable quartz resulting in a well-connected pore system with high permeability. Further mineralogical data show that the clay minerals present are in minor concentrations. Also, the position of the Yabraso and Bimbila Sandstones in the project area as plotted on the geological map show that there is a close proximity relationship between these sandstones and the limestones; hence forming a conducive system such that if hydrocarbons are produced by the possible source rocks (limestones), they can be housed by the sandstones.

Keywords: Volta Basin, Porosity, Permeability, Reservoir Rock, Bimbila Sandstone, Yabraso Sandstone

Introduction

Among the four sedimentary basins in Ghana (Tano Basin, Keta-Accra Basin, Saltpond Basin and Volta Basin), the least probed into for information on its hydrocarbon prospectivity is the Volta Basin. Unlike the Volta Basin, hydrocarbon exploration efforts were intensified on the other basins and their hydrocarbon prospectivity studied (Chudasama *et al*., 2016; Eisenlohr and Hirdes, 1992; Koffi *et al*., 2016; Leube *et al*., 1990; Milési et al., 1991; Smith *et al*., 2016).

The Volta Basin develops contact with the Birimian Supergroup of Ghana containing sediments dating from the Precambrian and Palaeozoic age (Affaton *et al*., 1991; Affaton *et al*., 1980; Anani, 1999; Kesse, 1984). A clearly defined petroleum system has not yet been established for the basin though studies on the basin have heightened in recent times especially as a result of the Ghana National Petroleum Cooperation's pioneering exploration activities in the basin called the Voltain Basin Project (VBP). Under this 5-year project (from 2015-2019), 2D seismic data was acquired, environmental assessments made and two conventional wells drilled with the objective of establishing prospectivity and enhancing the knowledge base of the basin (The Voltaian Basin Project, 2016). This was quite laudable and has made a frontier area available for increased exploratory activity. However, a huge gap in information pertaining to the rock types and their characteristics as source and reservoir rocks still remains to be studied. This will help infer the presence of a petroleum system suitable for hydrocarbon exploration and exploration work subsequently commenced to achieve the broader vision of the Volta Basin Project (VBP), which is to increase the hydrocarbon reserve base of the country. It is important to study the source and reservoir rock characteristic of the Volta Basin because the characteristics of the sedimentary rocks as source and reservoir is an indicator for determining the presence of petroleum (Adenutsi *et al.*, 2019; Quaye *et al*., 2023; Quaye *et al*., 2022; Sun *et al*., 2022; Toro *et al*., 2018; Yu *et al*., 2023; Zobah *et al*., 2022).

Romanian and Soviet geologist survey team, while drilling in the Volta Basin encountered viscous oily bitumen and oil sips in the drilled boreholes from the sandstone and the carbonate rocks of the basin especially at Nasia, Buipe and Yendi within the Oti member of the Volta Basin in the Northern parts of the country (Bozhko, 2008). This suggests that hydrocarbons may be present in the basin. This was not the only case of oil spills observed. During research by Boamah (2017), bitumen was also found in the quartz veins and carbonate rocks of the Buipe quarry (Boamah, 2017). Analysis by Abu *et al*. (2021) further confirmed that the limestones in the north-eastern region of the country are dolomitic and barite bearing due to hydrothermal mineralization of the carbonates (Abu *et al*., 2021). It is therefore necessary to study the porosities and permeabilities of the rocks within the Volta Basin to ascertain their potential as petroleum reservoir rocks.

In this study, the petrophysical properties of two sandstone formations namely the Yabraso and Bimbila Sandstones are studied. Furthermore, petrographic studies were also carried out on the microscopic scale to explain the observed petrophysical properties.

Materials and Methods

The study employed the application of field and laboratory techniques to investigate reservoir rocks characteristics. The

*Corresponding author: casdanad@hotmail.com

[1] Department of Geological Engineering, Faculty of Civil and Geo-Engineering, Kwame Nkrumah University of Science and Technology, Kumasi, Ghana

[2] Department of Petroleum Engineering, Faculty of Civil and Geo-Engineering, Kwame Nkrumah University of Science and Technology, Kumasi Ghana

[3] Department of Physics, Faculty of Physical and Computational Sciences, Kwame Nkrumah University of Science and Technology, Kumasi Ghana

field method used in the study is the geological mapping of outcrops with a representative sub-surface sampling. The laboratory techniques employed are the petrographic, petrophysical, and mineralogical analysis. The field sheet of the study area (Field sheets 1002D1 and part of 1002D3) encompassing the North East and Upper East Regions of Ghana, specifically the Mamprugu-Moagduri District and Builsa South District were obtained from the Geological Survey Department of Ghana. The field sheets cover Ghana's latitudes 9°55'N and 10°35'N and longitudes 0°35' W and 1°45' W.

Field mapping

A thirty-day field mapping exercise was conducted in the Mamprugu-Moagduri District. Each day involved traversing over the pre-determined traverse route, noting the geology on the way and picking samples where necessary. Where rivers and streams were encountered, mapping was possible by crossing or finding another route to access the geological information needed.

Locality names and sample names were given on the field to identify the different samples taken. Attitudes (strike and dip) of rocks, observed mineralogy and textures and physical features were also noted.

Geology of the study area

The rock types observed in the filed were noted to be some silexites, sandstones, siltstones, mudstones, limestones, volcaniclastics and some granitoids (see Figure 1). It is however noteworthy that only the sandstones are considered in detail in this study hence the other rock types encountered are not discussed. Two main formations necessary to this study as identified in the field were the Yabraso Formation observed mainly at the edge of the basin and the Bimbila Formation observed at the core of the Basin.

Silexites, sandstones, weakly micaceous siltstones and mudstones as well as carbonate rocks constituted the Bimbila Formation. Volcaniclastics, metasediments, and granitoids of the Birimian Supergroup were observed to underlie the sedimentary units of the Volta Basin during the mapping exercise. Volcaniclastics were seen from the Brahmahabofuo river through to Fumbisi Bachisa and also mainly at Nangruma (gold mining community). They were seen as dipping NW and highly sheared but not weathered like the observed metasediments. They are less dense/hard and foliated with strike of foliation being 045º.

Petrophysical analysis

Petrophysical analysis was conducted to determine the porosity of the Yabraso Sandstone and the Bimbila Sandstone. The porosity values where then used in correlation to compute the permeability values. The samples were cored using a manual drill press and some of the Bimbila sandstone samples showed fractures upon coring (see Figure 2). The drilling bit used was the diamond drill and the core diameter was 1.5 inches. After drilling, the drill bit was dismounted and the core retrieved. A total of twenty-two (22) retrieved cores were trimmed to smooth and even surfaces and the desired sizes, using the Single Trim Saw. Ten of the samples where Bimbila Sandstones and the remaining twelve where Yabraso Sandstones. The dimensions of the samples were measured and the dry weight of the samples was determined with an electronic balance before the porosity test was conducted.

Effective porosity determination was done by the use of the Helium Porosimetry method. The Timur's (Timur, 1968) and

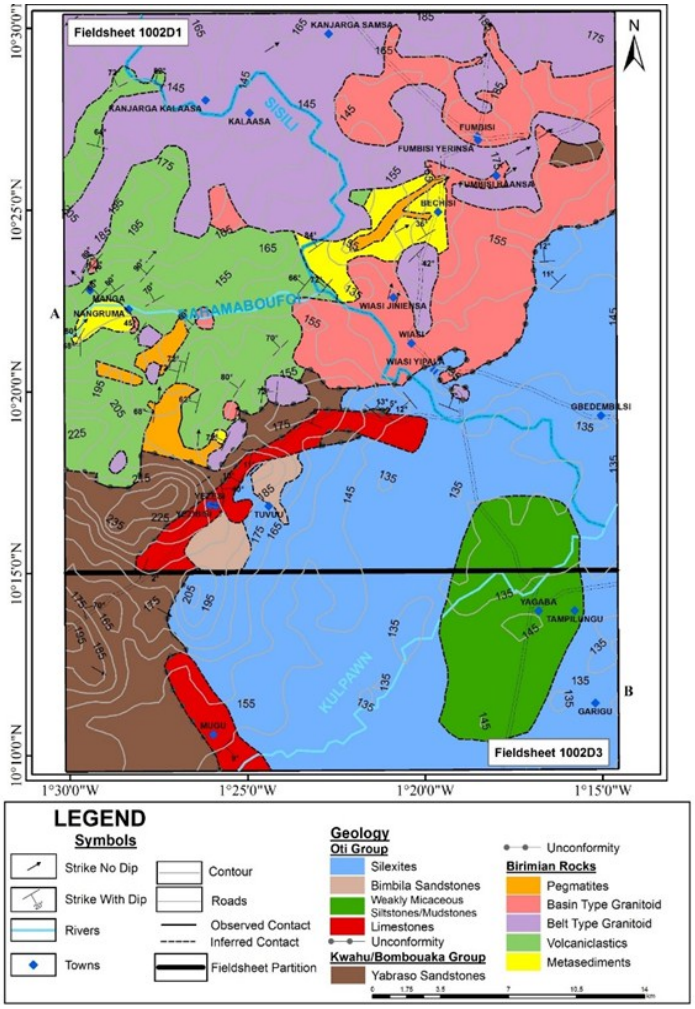

Figure 1 Geological map of the project area

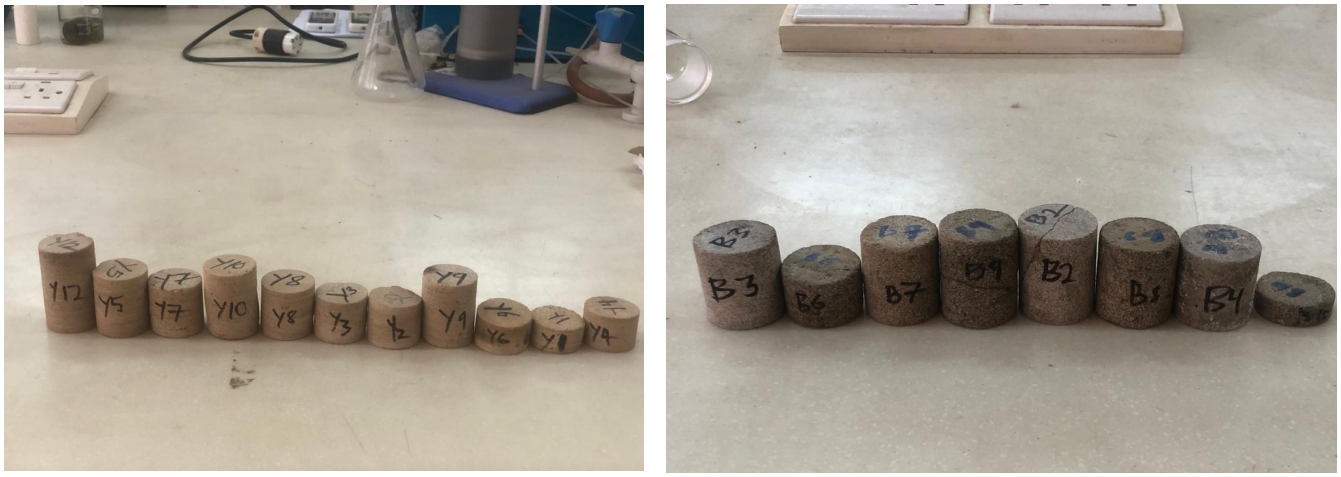

Figure 2 Core samples of (a) Yabraso sandstones and (b) Bimbila sandstones

Morris-Bigg's (Ahmed, 2018; Dayanım *et al.*, 2017) correlations were used in estimating permeability. Fluid productive sandstones typically have porosity values of 5 % to 40 % (Guo *et al.*, 2014) and permeability range of 100 to 500 mD with fractures having infinite permeability (Magoon, 2004; Satter and Iqbal, 2015; Tiab and Donaldson, 2015).

Per the qualitative assessment of porosity (Becker *et al.*, 2017; Timur, 1968), average porosities of 0-5 % is negligible, 5-10 % (poor), 10-20 % (good), 20-30 % (very good) and above 30 % (excellent) and the quality of a reservoir as determined by permeability, in mD, may be judged as poor if $k<1$, fair if $1<k<10$, moderate if $10<k<50$, good if $50<k<250$, and very good if $k>250$ mD (Tiab and Donaldson, 2015).

Twelve (12) Yabraso sandstone plugs and Ten (10) Bimbila sandstone plugs were analyzed for effective porosity using helium gas. The corresponding bulk volume (V_b) and effective porosity ($\emptyset_\epsilon$) of the sandstones using helium gas were also determined using equations 1 and 2, respectively.

$$V_b = \pi\left(\frac{d}{2}\right)^2 h \quad (1)$$

$$\phi_e = \frac{V_b - V_g}{V_b} \quad (2)$$

Where V_b is the bulk volume, d is the diameter of core plug, h is height of core plug, $\emptyset_\epsilon$ is the effective (interconnected) porosity of the core plug and vg is the grain volume. The corresponding permeability values of the sandstones were determined through correlation using the Eqn (3) by Timur (1968) whereas Morris-Biggs correlation (Eqn. (4)) used to cross check the permeability values (Ahmed, 2018).

$$k = \frac{0.136(\phi_e)^{4.40}}{S_{wc}} \quad (3)$$

$$k = \frac{C(\phi_e)^8}{S_{wc}} \quad (4)$$

Where, k is permeability and C is 80 for gas and 250 for oil and S_{we} is connate water saturation. A connate water value of 0.2 was assumed and Helium gas was used for the permeability measurement hence the C value used is 80.

Petrographic analysis

This entailed the description and naming of the sedimentary rocks following protocols of Schnurrenberger *et al.* (2003), sample preparation, observation of thin sections prepared to 30 microns under a petrographic microscope and description of the physical (grain size, texture, arrangement, sorting, pleochroism, relief, birefringence, opaque minerals etc.) and mineralogical properties of the samples (Reineck and Singh, 2012; Schnurrenberger *et al.*, 2003). Samples were examined using cross hairs or crossed polarized light (XPL) and plane polarized light (PPL).

A total of thirty (30) samples were prepared for petrographic analysis. The Hillquist Slab Saw and Trim Saw were used to cut slabs out of the field sample. The slabs were further trimmed using the Trim saw to ensure that no cut face was protruding and there was uniformity and evenness.

Thin section preparation was done in two stages. The coarse grinding and the fine grinding. During the coarse grinding, the slabs were smoothened on abrasives silicon carbide paper from the 400 paper (roughest) through to the 1200 paper (smoothest). The glass slides were prepared for bonding by frosting using the 220 microns silicon carbide powder. The frosted glass slide was washed, dried and set up for bonding. The best face of the rock slab was carefully selected and lapped. After bonding, fine grinding was then done by first grinding the bonded slabs with the Hillquist Trim to about 60 microns and then further reducing it to 30 microns during finishing using the Hillquist Polishing Grinder. The 30-micron mark was achieved by observing the slide under a microscope during grinding till no interference colour is spotted. EpoResin was used for bonding the best face of the slab to the frosted glass slide using the ratio, 15 ml of epofix resin is to 2 mils of epofix hardener. After 48 hours, the slide was well bonded, and finishing was done.

Ten samples were separately prepared through cutting to trimming. They were then bonded and stained with blue dye for 24 hours before grinding to 30microns and finishing. These stained sandstones were observed for porosity and permeability interpretations under the petrographic microscope. The samples were mounted on the Leica DM 750P and Leica DM 4P transmitted light petrographic microscope and observed for their physical and mineralogical properties. Various minerals are identified using the Michel-Levy Birefringence Chart and its corresponding mineral classes.

Mineralogical analysis

The method for mineralogical analysis employed was the X-ray diffraction. The samples were crushed to sixty-three (63) microns. In this method, a material is radiated with an incident x-ray to measure its intensity by scattering angles of the x-ray leaving the material. This helps to determine the crystallographic structure of the material and hence determine the minerals present. The minerals present are determined when the crystals scatter the incident x-ray through interaction with atoms' electrons. The scatter produces an array of spherical waves and show a specific direction to determine the intensity of the mineral present through Bragg's law (Bunaciu *et al.*, 2015; Zhang *et al.*, 2019).

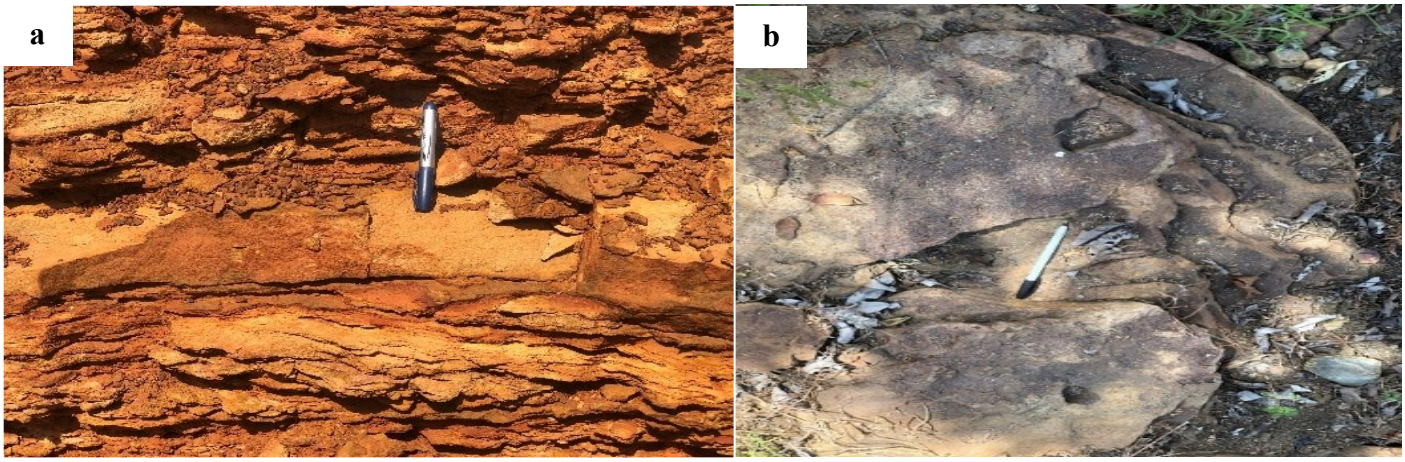

Figure 3 Examples of (a) Yabraso Sandstones and (b) Bimbilla Sandstones observed in the study

Table 1 Bulk volume, permeability (k) and effective porosity of Yabraso sandstone core plugs under helium gas

Core ID	Diameter (cm)	Length (cm)	Bulk Volume (cm^3)	Grain Volume (cm^3)	Effective Porosity (%)	k (Timur), mD	k (Morris-Biggs), mD
Y1	3.77	1.92	21.43	16.70	22	274.24	177.15
Y2	3.79	3.26	36.77	31.44	14	37.53	11.76
Y3	3.76	3.26	36.19	31.44	13	27.09	7.54
Y4	3.77	2.73	30.47	24.49	19	143.87	73.50
Y5	3.78	4.65	52.18	45.99	11	12.98	2.76
Y6	3.79	2.90	32.71	24.65	24	402.16	298.59
Y7	3.79	3.92	44.22	40.72	7	1.77	0.18
Y8	3.77	3.97	44.31	37.83	14	37.53	11.76
Y9	3.78	5.04	56.55	51.05	9	5.37	0.83
Y10	3.73	5.28	57.69	51.05	11	12.98	2.76
Y11	3.71	5.85	63.24	57.71	8	3.19	0.40
Y12	3.75	6.35	70.13	61.73	11	12.98	2.76
Arithmetic Mean					**13**	**63.41**	**49.17**

Results and Discussion

Field Observation

The Yabraso Sandstones (see Figure 3a) were yellowish/ brownish in colour, fine to medium grained, flaggy, quartzose, and cross-bedded. They outcrop in and around Yezizi, Yezibizi, and the outskirts of Nandem with general strike values of 075º. The Bimbila Sandstones were observed as grayish to dark colored, slightly massive rocks occurring as pockets in limestone areas and reacting with dilute HCl (see Figure 3b).

The porosity values range from 7 to 24 % (poor to very good) with an average porosity of 13 % (Good) shows that the Yabraso Sandstone has a good porosity (Guo *et al*., 2014). A permeability of 63.41mD and 49.17mD imply that the Yabraso sandstone has a moderate to good permeability range since sandstones are moderate if 10<k<50 and good if 50<k<250 (Tiab and Donaldson, 2015).

The corresponding poro-perm plots for Timur (see Figure 4a) and Morris-Biggs (see Figure 4b) show that permeability increases with porosity. The porosity and permeability values (see Table 1) are represented in bar graphs (see Figures 5, 6a and 6b). Porosity range for Yabraso sandstone samples (see Figure 5) show that three (3) samples fall within the range of poor porosity (5-10%), seven (7) samples have good porosity (10-20%) and only two (2) samples have very good porosities (20-30%).

Permeability range of the Yabraso Sandstone samples for Timur correlation (see Figure 6a) show that three (3) samples have fair permeability (1-10 mD), six (6) samples have moderate permeability (10-50 mD), one (1) sample has good permeability (50-250 mD) and two (2) samples have very good permeability (above 250 mD) and for Morris-Biggs correlation (see Figure 6b), three (3) samples have poor permeability (Below 1 mD), four (4) samples have fair permeability (1-10 mD), two (2) samples have moderate permeability (10-50 mD), two (2) samples have good permeability (50-250 mD) and one (1) sam-

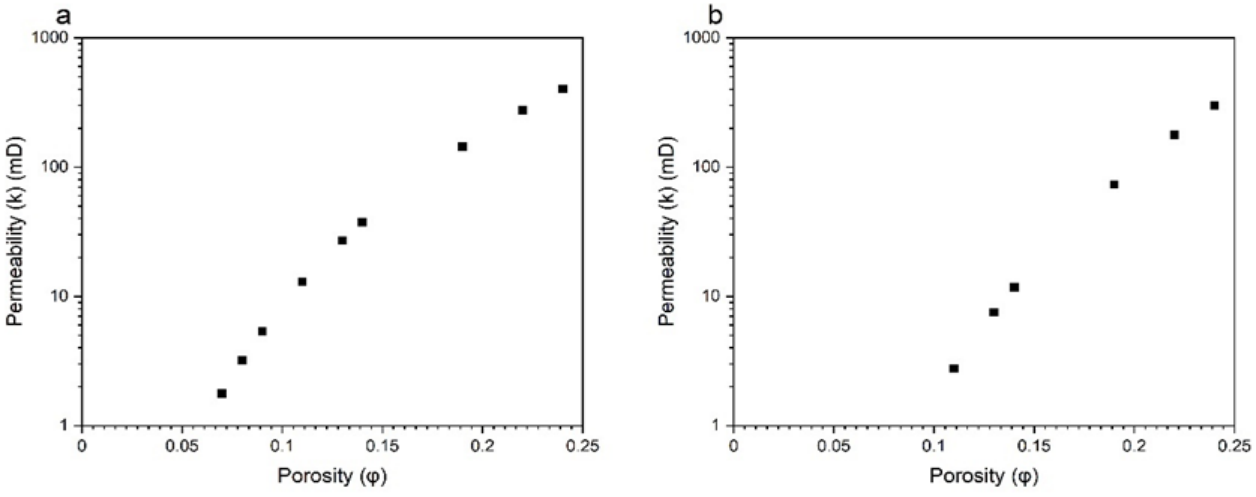

Figure 4 (a) Timur and (b) Morris-Biggs porosity-permeability plots for Yabraso Sandstones

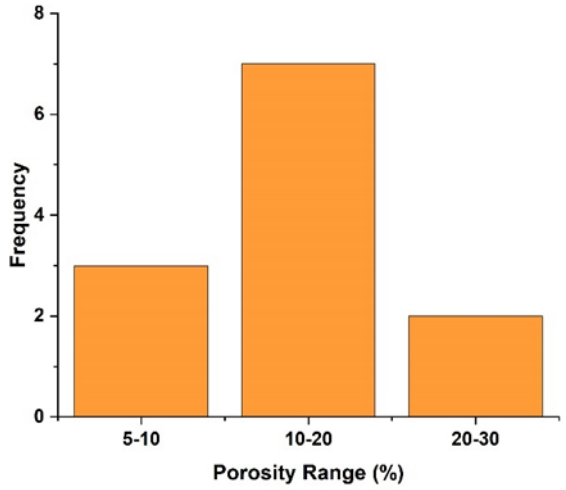

Figure 5 Porosity range for Yabraso sandstone samples

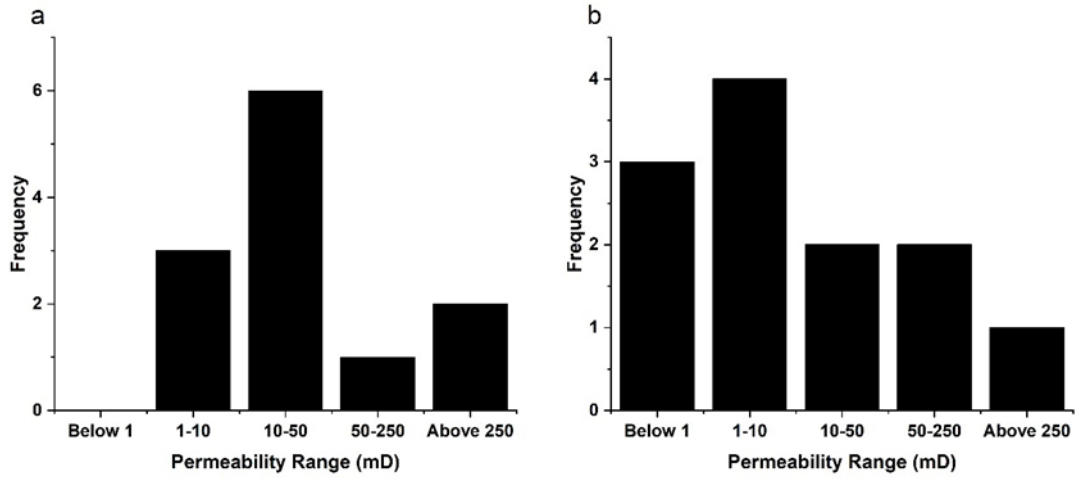

Figure 6 Permeability range of Yabraso Sandstones for (a) Timur and (b) Morris-Biggs correlations

Table 2 Bulk volume, permeability (k) and effective porosity of Bimbila sandstone core plugs under helium gas

Core ID	Diameter (cm)	Length (cm)	Bulk Volume (cm^3)	Grain Volume (cm^3)	Effective Porosity (%)	k (Timur), mD	k (Morris-Biggs), mD
B1	3.79	4.85	54.71	50.93	6	0.90	0.07
B2	3.80	5.24	59.42	55.46	6	0.90	0.07
B3	3.80	4.48	50.80	45.99	9	5.37	0.83
B4	3.85	3.30	38.41	34.85	9	5.37	0.83
B5	3.80	2.25	25.51	21.07	17	88.19	37.71
B6	3.78	2.89	32.43	24.80	23	333.48	231.30
B7	3.77	4.73	52.79	40.73	22	274.24	177.15
B8	3.86	4.68	54.76	43.46	20	180.30	100.00
B9	3.87	5.19	61.04	46.07	24	402.16	298.59
B10	3.78	1.33	14.92	12.89	13	27.09	7.54
Arithmetic Mean					**14**	**131.80**	**85.41**

ple has very good permeability (above 250 mD).

The porosity values range from 6 % (poor) to 24 % (very good) with an average porosity of 14 % (Good) which indicates that the Bimbila Sandstone has good porosity (Guo *et al*., 2014). The corresponding permeability values (see Table 2) of the Bimbila sandstones were determined through correlation using Timur and Morris-Biggs equations. A permeability of 131.80 mD imply that the Bimbila sandstone has a good permeability since sandstones should have a permeability of 100 to 500 mD (Tiab and Donaldson, 2015).

The corresponding poro-perm plots for Timur (see Figure 7a) and Morris-Biggs (see Figure 7b) show that permeability increases with porosity. The porosity and permeability values (see Table 2) are represented in bar graphs (see Figures 8, 9a and 9b). Porosity range for Bimbila sandstone samples (see Figure 8) show that four (4) samples fall within the range of poor porosity (5-10 %), two (2) samples have good porosity (10 -20 %) and four (4) samples have very good porosities (20-30 %).

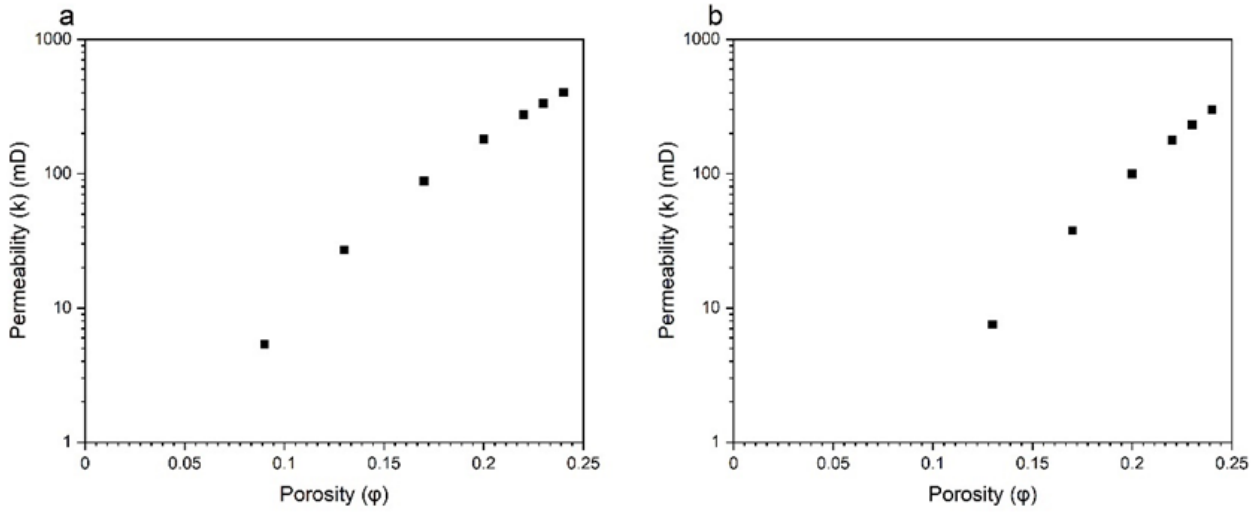

Figure 7 (a) Timur and (b) Morris-Biggs porosity-permeability plots for Bimbila Sandstones

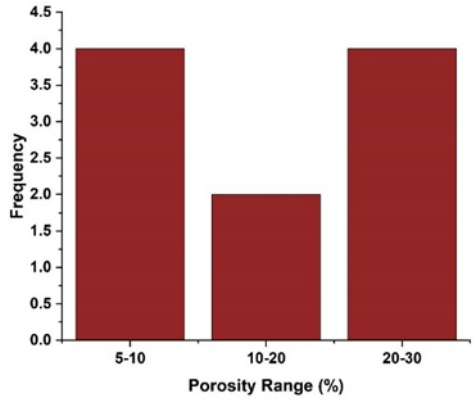

Figure 8 Porosity range for Bimbila sandstones

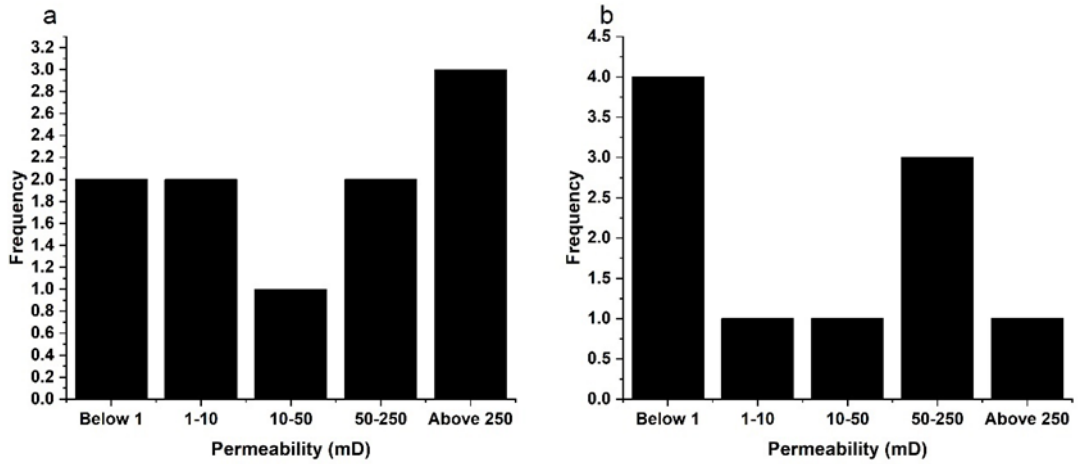

Figure 9 Permeability range of the Bimbila sandstones for (a) Timur and (b) Morris-Biggs correlations

Permeability range of the Bimbila Sandstone samples for Timur correlation (see Figure 9a) show that two (2) samples have poor permeability (Below 1 mD), two (2) samples have fair permeability (1-10 mD), one (1) sample has moderate permeability (10-50 mD), two (2) samples have good permeability (50-250 mD) and three (3) samples have very good permeability (above 250 mD) and for Morris-Biggs correlation (see Figure 9a), four (4) samples have poor permeability (Below 1 mD), one (1) sample has fair permeability (1-10 mD), one (1) sample has moderate permeability (10-50 mD), three (3) samples have good permeability (50-250 mD) and one (1) sample has very good permeability (above 250 mD).

Petrographic Analysis

Petrographic analysis of the Yabraso Sandstones

The Yabraso Sandstone observed under the petrographic microscope (xpl, x4) are composed of quartz (Qz), muscovite (Ms), biotite (Bt), limonite (Lim) and lithic fragments (see Figure 10) making up the framework grains. There are little to zero matrix content, with ferroan cement as the main cementing material (See Figure 10). The quartz grains are medium grained, and subangular to subrounded (see Figure 10c) and moderately to poorly sorted. The Yabraso Sandstones occur as both monocrystalline and polycrystalline types.

The polycrystalline grains suggest that the rocks after being under some stress (either tectonic or metamorphic) encountered strain which partitioned the crystal framework thereby distorting the crystal lattice causing the once monocrystalline quartz to become polycrystalline. The quartz grains in most cases are conchoidally fractured and display a general undulatory extinction with some of the quartz grains having sutured boundaries (see Figure 10b and d). The suturing among quartz grains indicates incipient metamorphism asserting that metamorphism is just about taking place in the rock. Muscovite and biotite occur as random tiny fragments and/or elongated flakes, that are in some cases bent (see Figure 10). They are, however, mostly interstitial between quartz grains (see Figure 10).

These Yabraso sandstones may be considered texturally mature due to the presence of little or no matrix, dominance of rounded grains and the moderate sorting (see Figure 10). The mean modal analysis by visual estimation (see Table 3a) further confirmed the average percentage of quartz as 75 %, iron cement as 15 %, mica as 3 % and lithic fragments as 2 % based on relations thereby confirming that the rock is a sedimentary rock and a sandstone (Terry and Chilingar, 1955).

The Yabraso Sandstones stained with blue dye and observed under plane polarized light showed the pores (voids in the rocks) being filed with the blue dye (see Figure 11). The flow of the blue dye from pore to pore also shows the connectivity of the pore hence inferring the extent of permeability of the samples. Intraparticle pores (intraP) and interparticle pores (interP) are the pore systems observed for the Yabraso Sandstones under the microscope (see Figure 11a and b). They account for about 70% and 30% of the total porosity, respectively. Slit and wedge-shaped pores (see Figure 11c) are the major pore shapes observed.

These pores are seen to have good openness that can facilitate the storage of hydrocarbons and are also observed to be interconnected to each other by flow of the blue dye from pore to pore (see Figures 11d, e and f) thereby suggesting that they can be ease of flow/migration of hydrocarbons if any. Pore size diameters are mainly distributed in ranges of 100-500 µm.

Petrographic analysis of the Bimbila sandstones

The Bimbila Sandstones contain lithic fragments, iron oxides, muscovite, quartz (Qz), plagioclase, and K-feldspar. The rock's framework grains are made up of quartz, plagioclase, muscovite, K-feldspar, and lithic fragments (see Figures 12 and 13). There are little to zero matrix content, with ferroan cement as the main cementing material (see Figure 12). The rock may be considered texturally mature due to the presence of little or no matrix, dominance of rounded grains and moderate sorting.

The quartz grains (see Figure 13a, d, f and e) are coarse to medium grained, and subangular to subrounded. They occur as

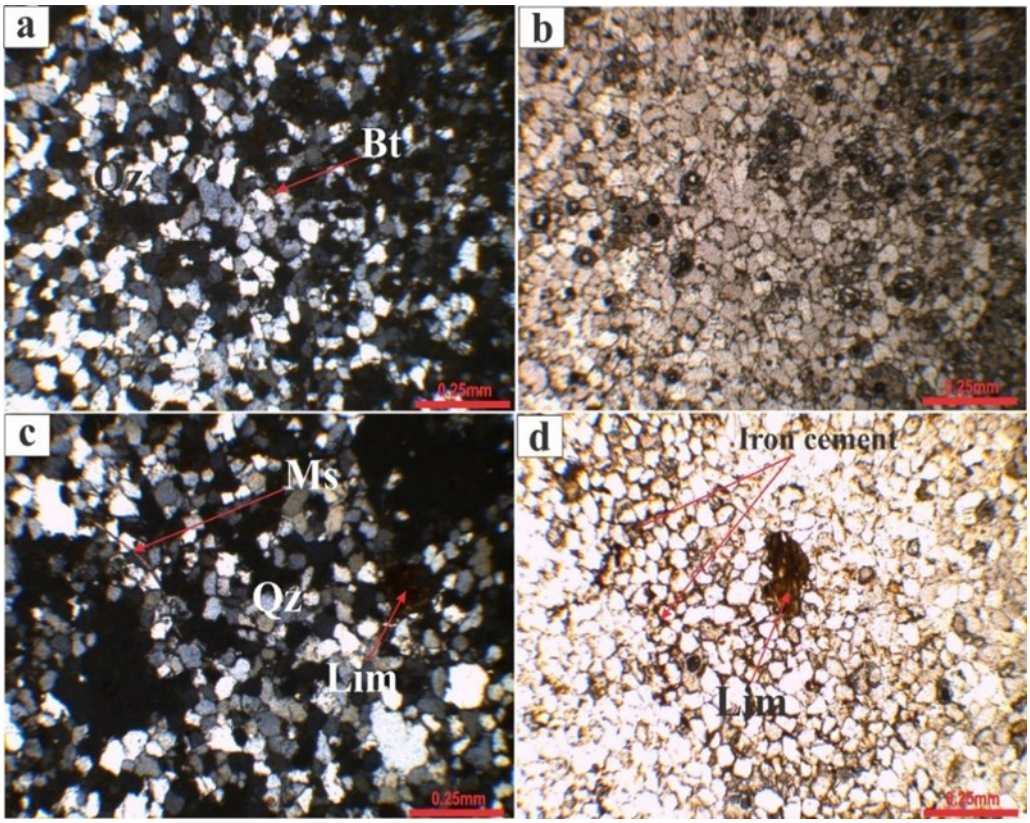

Figure 10 Medium to fine grained, moderately to poorly sorted Yabraso Sandstone (Y2)

both monocrystalline and polycrystalline types. The quartz grains typically exhibit conchoidal fractures and an overall undulatory extinction. There are quartz overgrowths on some of the quartz grains (see Figure 13b). With poorly preserved twin lamellae, the medium-grained plagioclase grains are subangular to subrounded. They are mainly the oligoclase type plagioclase. The K-feldspar grains are medium grained and subangular to subrounded, with the occurrence of both orthoclase and microcline types (see Figure 13b).

Muscovite occurs as random tiny fragments and/or elongated flakes. They are however, mostly interstitial between quartz grains. The lithic fragments occur as ironic cherts and volcanic rocks (see Figure 12a). Suturing among quartz grains indicate incipient metamorphism. The mean modal analysis by visual estimation is shown in Table 3b based on Terry & Chilingar (1955), confirming that the rock is a sedimentary rock and a sandstone (Terry and Chilingar, 1955).

The Bimbila Sandstones stained with a blue dye and observed under plane polarized light show the pores (voids in the rocks) as those filled with the blue dye (see Figure 14). The flow of the blue dye from pore to pore also shows the connectivity of the pore hence inferring the extent of permeability of the samples. Two pore systems are observed, intraparticle pores (intraP) and interparticle pores (interP) slit and wedge-shaped pores are the major pore shapes observed (see Figure 14b and c).

These pores have good openness that can facilitate the storage of hydrocarbons. Furthermore, the pores are seen to be interconnected to each other (see Figure 14a and b) thereby facilitating ease of flow/migration of hydrocarbons if any. Pore size diameters are mainly distributed in ranges of 200-500 μm.

QFL Ternary plots

To classify the Yabraso and Bimbila Sandstones, the minerals present are grouped into three (Q being the quartz, F being the Feldspars and L being the lithic fragments (Folk, 1974). The ternary plots (see Figures 15a and 15b) show that both Sandstones are sub-arkose to quartz arenites,

Mineralogical analysis

The coupled two theta x-ray diffractometer tests on the Yabraso Sandstone samples revealed that the only clay mineral present is Kaolinite and it occurs in minor concentration level of 1.7%.

Table 3 Mean modal composition of (a) Yabraso and (b) Bimbila sandstones via visual estimation based on Terry & Chilingar (1955)

(a) Yabraso Sandstone

Mineral	Modal Composition %
Quartz	75
Iron cement	5
Feldspar	17
Muscovite + Biotite	3

(b) Bimbila Sandstone

Mineral	Modal Composition %
Quartz	71
Iron oxide	20
Plagioclase	2
K-feldspar	3
Muscovite	2
Lithic fragment	2

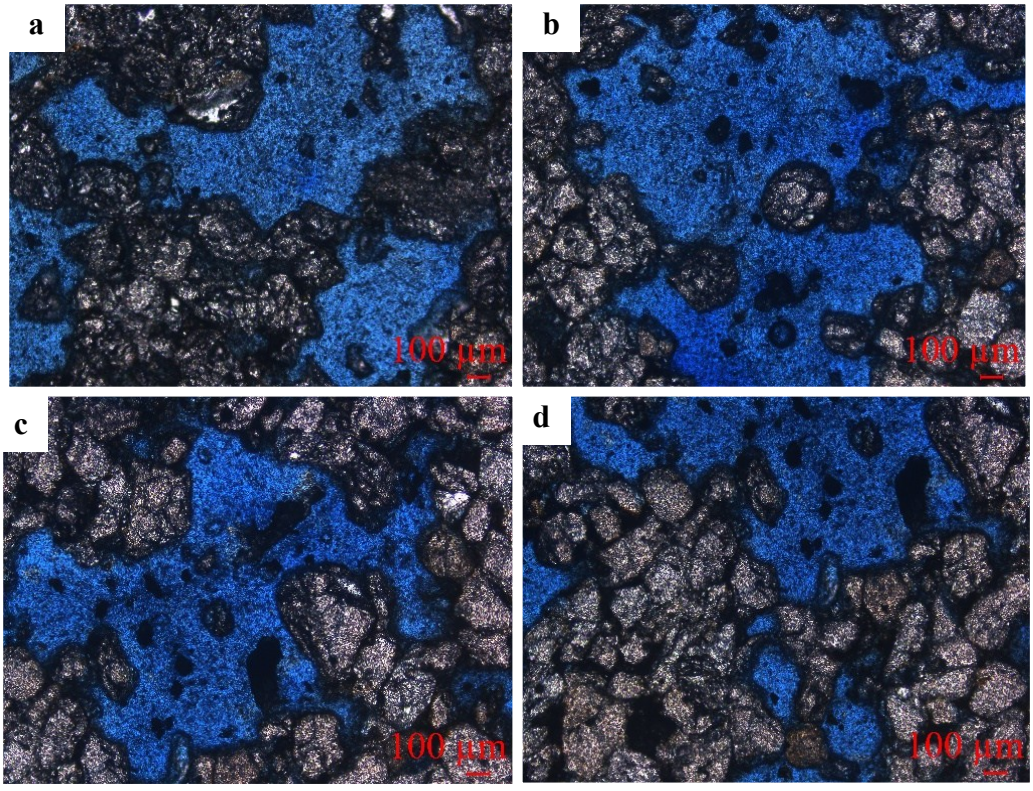

Figure 11 Stained Yabraso sandstones (Y2) under ppl (x4); (a-d) showing pore filling of blue dye

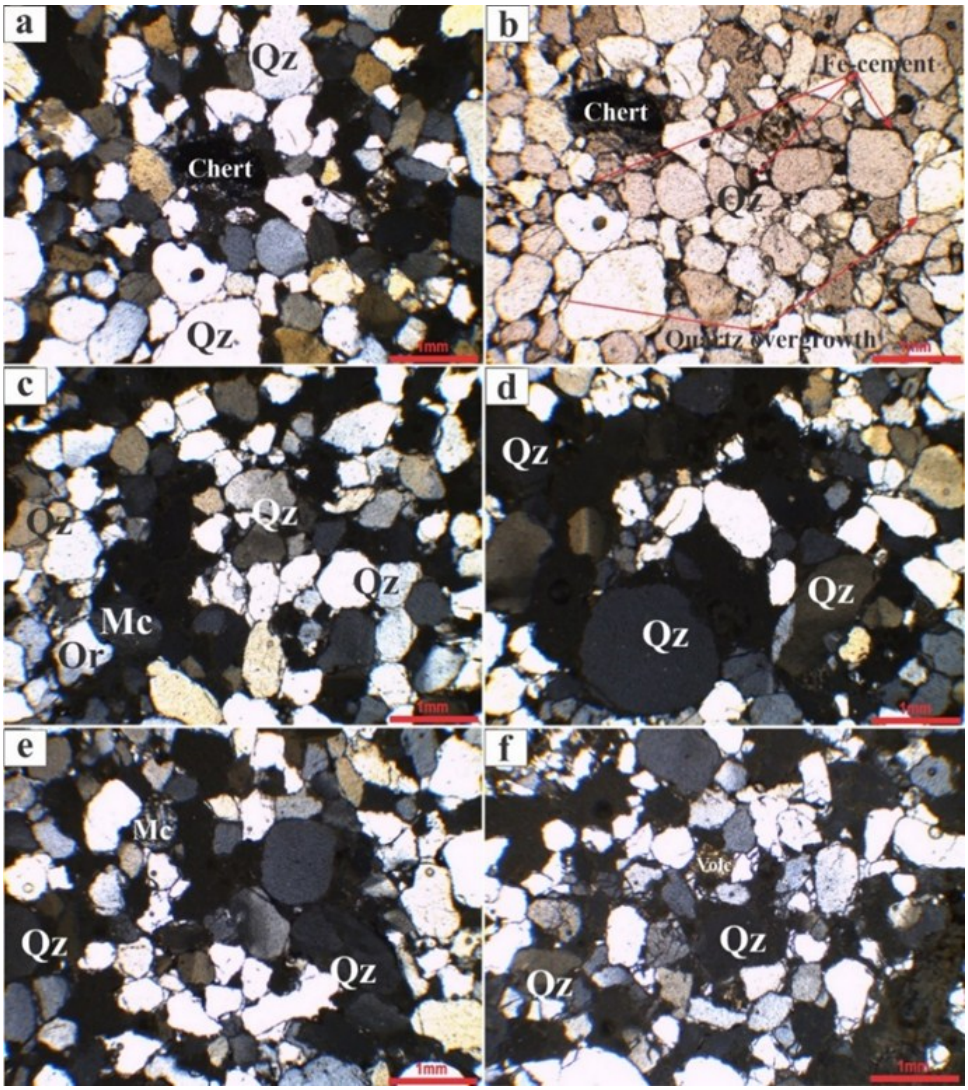

Figure 12 Medium to fine well sorted Bimbila Sandstones (B4) showing (a-f): iron cement, quartz overgrowth and well-rounded grains

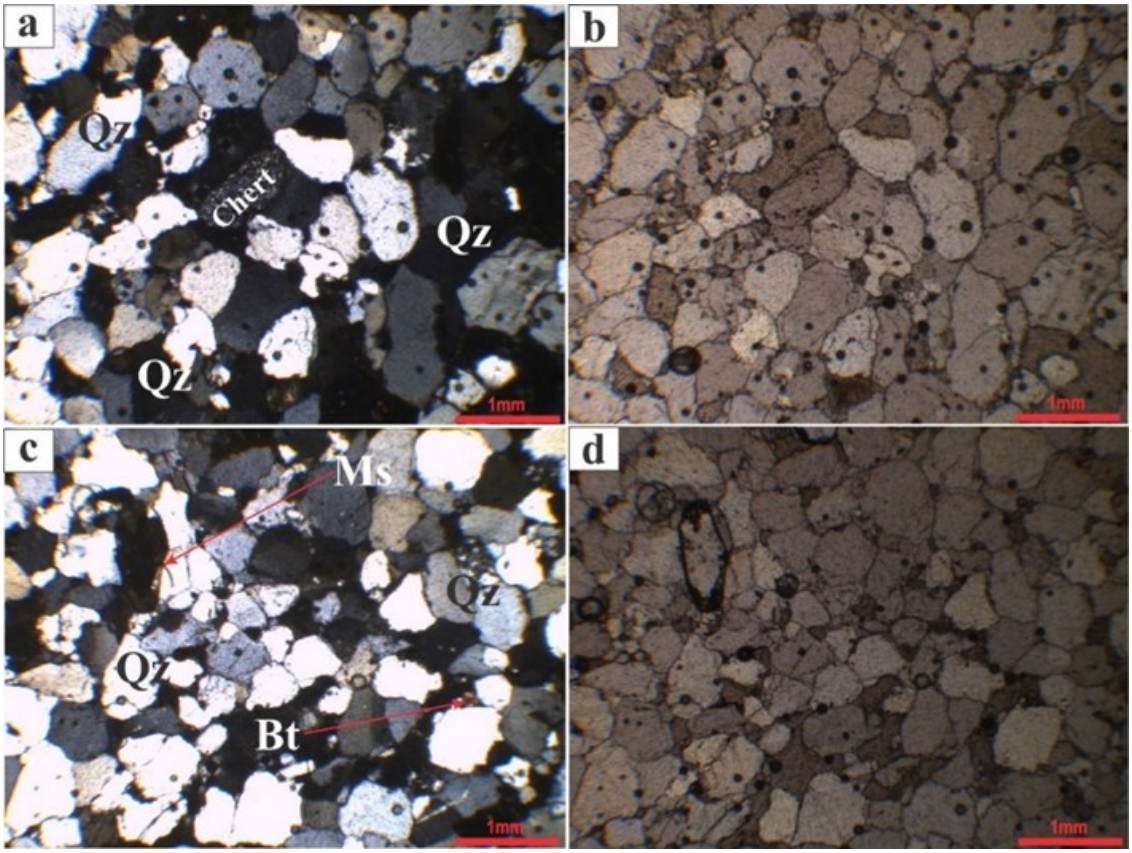

Figure 13 Bimbila Sandstone (B5) showing (a-d): minerals and chert lithic fragments

The other minerals present were Quartz (35.4 %), Lepidote (0.5 %), Mica (27.7 %), Microcline (16.2 %), Orthoclase (18.1 %) and Burkeite (0.4 %) as represented in Figure16a. Since the clay mineral present is not in major quantities, it may not be of negative effect to the reservoir rock quality, thus suggesting the Yabraso Sandstone may be a good reservoir rock.

For the Bimbila Sandstone samples, it revealed that the only clay mineral present is Kaolinite and it occurs in minor concentration level of 3.0 % which may not be of negative effect to the reservoir rock quality, thus suggesting the Bimbila Sandstone may be a good reservoir rock. The other minerals present are Quartz (68.8 %), Fourmarierite (0.3 %) and Microcline (27.9 %) as presented in Figure 16b.

The Yabraso sandstones as observed under the microscope have finer subangular to angular grains (see Figure 10) as compared to the Bimbila Sandstones which shows more medium subrounded to rounded grains (see Figure 12, 13 and 17). It is presumed that these grain shapes in the Yabraso and Bimbila Sandstones constitute a driving force behind the smaller quartz abundances in the rock samples. Following discussions by Heap *et al*. (2016), higher permeability is induced by larger grain size (Heap *et al*., 2017). This is evident in the studied stained Bimbila Sandstones as the more medium to fine grain structures showed more ease of spread of the blue dye through the pores (see Figure 14) and their connectivity from pore to pore (permeability), as compared to the Yabraso Sandstones (see Figure 11).

Grain sorting sorting improves reservoir quality since it results in larger packing-induced porosities (McKinley *et al*., 2011). The samples studied under the microscope showed a

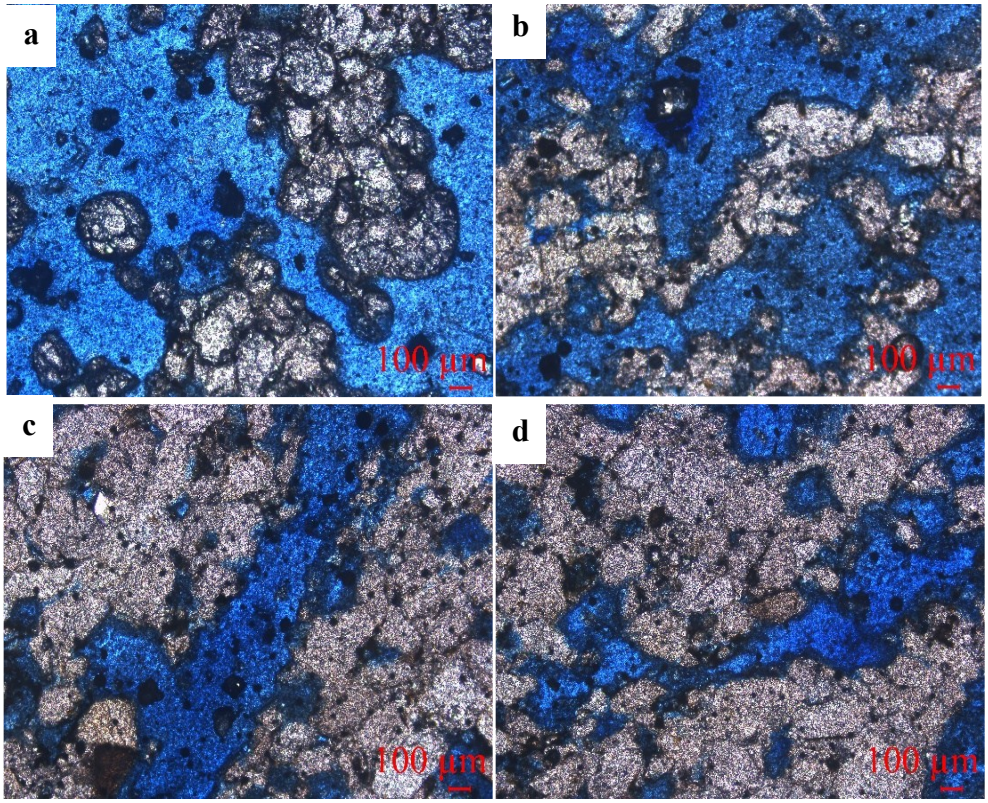

Figure 14 Stained Bimbila sandstone a-d showing pore filling and pore connectivity (ppl, x5).

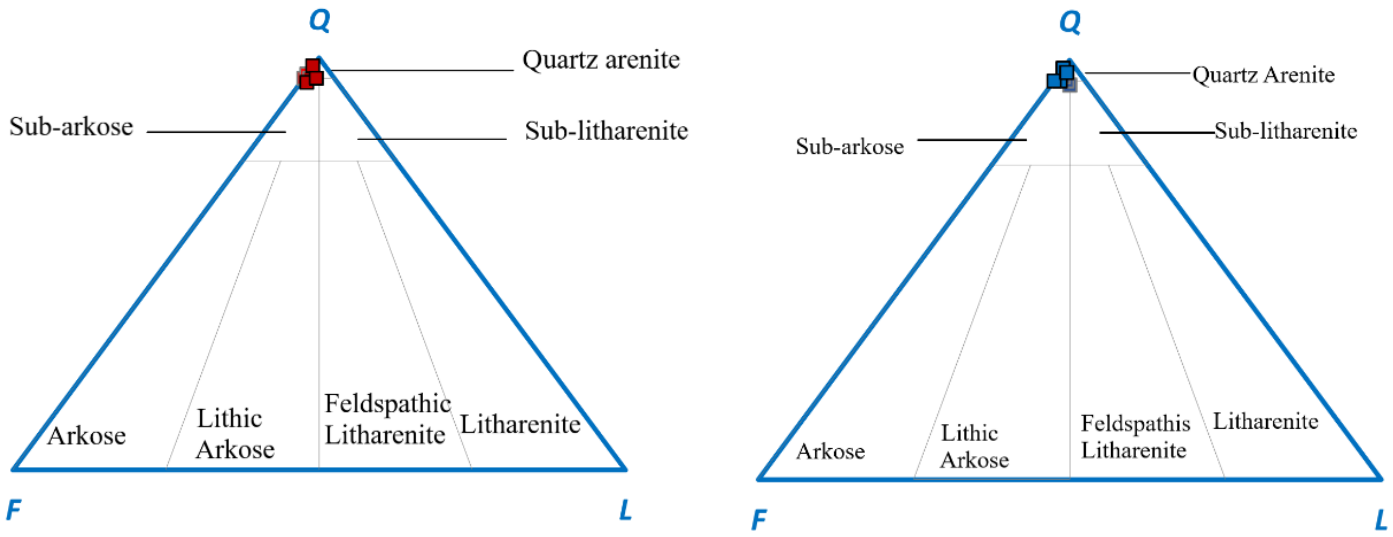

Figure 15 Ternary plot generated for the (a) Yabraso and (b) Bimbila sandstones

better sorting for the Bimbila sandstones (see Figure 18b); hence, it can be inferred that there is a packing induced porosity for the Bimbila rocks, which leads to the observation of a higher porosity of 14 % in the Bimbila rocks during petrophysical evaluation (see Figure 12, 13 and 14).

The examined samples showed coats of iron oxide and clay minerals (see Figure 10 and 12). This may have originated as a result of iron-bearing sediments reddening during weathering by minerals such as hornblende and biotite (Walker and Honea, 1969). Grain migration may be the root cause of the sandstones' varying grain coatings and clay mineral distribution (Ajdukiewicz *et al*., 2010), where the clay coatings could only be retained by the smaller grains. This agrees with the observations made under the microscope for the Yabraso sandstones, which shows clay coats mostly preserved on smaller grains (see Figure 10).

Due to the fact that feldspar is not stable under the pH values present in meteoric waters (Yuan *et al*., 2015), feldspar dissolution may have created the intragranular feldspar porosity in the sandstone samples (see Figure 10 and 12) which may have started pre-deposition. It must have developed in these samples prior to illitization, most likely during early diagenesis (Becker *et al*., 2017).

Illite grain coatings (see Figure 10) observed at grain contacts must have existed before mechanical compaction. In active eolian depositional systems, illite clays as grain coatings have also been reported as a detrital to diagenetic component (Busch, 2020).

Compaction reduce porosity and permeability because it causes grain rearrangement and plastic deformation of ductile grains which will fill the pores and pore throats (Dos Anjos *et al*., 2000; Griffiths *et al*., 2018; Morad *et al*., 2010; Worden *et al*., 2000). Cementation due to the precipitation of authigenic minerals reduces reservoir quality (Monsees *et al*., 2021; Rossi *et al*., 2002). However, some authigenic minerals can retain their initial porosity during early deformation by preventing the rock from deteriorating due to compaction or cementation (Grier and Marschall, 1992). Cementation due to the precipitation of authigenic minerals (limonite) was observed in the Yabraso sandstone samples studied because the authigenic mineral (limonite) was seen to be deforming thus, subrounded to subangular (see Figure 10). Pore-filling illite and quartz in Sandstones being abundant (see Figure 10) may be interpreted as being due to the unconformity between the Birimian Rocks and the Volta Basin (see Figure 1). A similar phenomenon is identified in the Northern German Basin (Legler *et al*., 2011).

In the sample set under study, effective helium porosity shows porosity range of 7-22 % with an average value of 13 % in the Yabraso sandstones and a range of 6-24 % with an average porosity of 14 % for the Bimbila Sandstones and permeability values of 63.41 mD and 131.80 mD respectively. Though the porosity values of 13 % and 14 % shows that the rocks have a good fluid holding capacity (porosity), the permeability (fluid transmission) values show clearly the Bimbila Sandstones have more fluid transmissivity capability than the Yabraso Sandstones which has a fluid transmissivity (permeability) value of

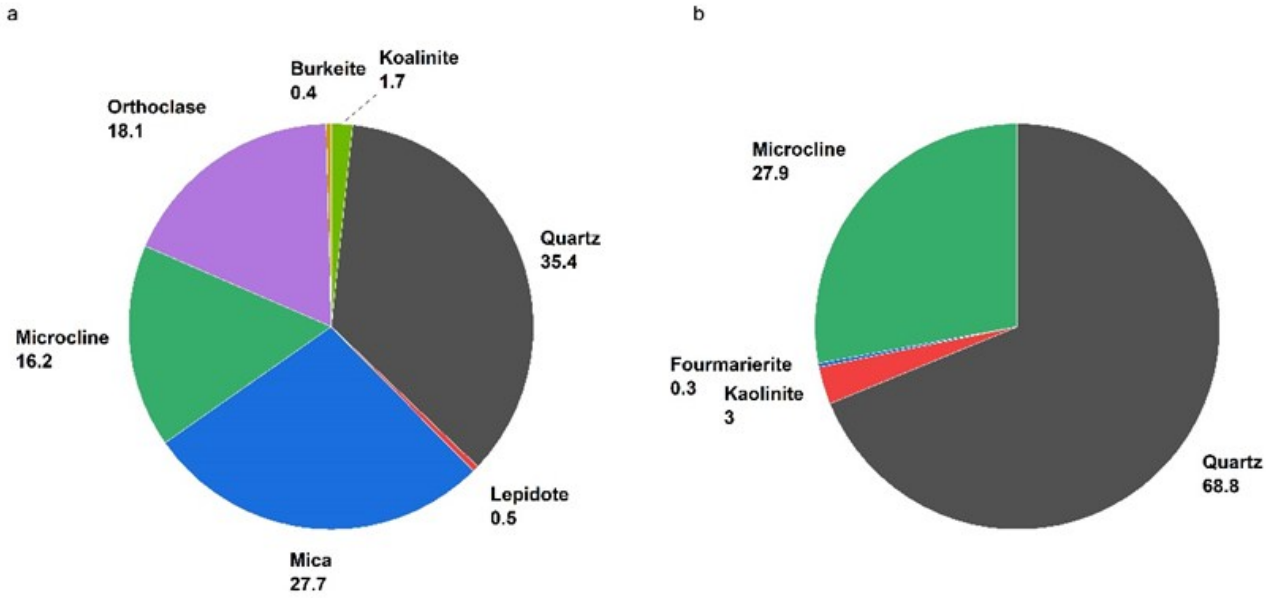

Figure 16 XRD mineral concentrations of (a) Yabraso and (b) Bimbila sandstones

Table 4 Summary of petrographic analysis conducted on Yabraso and Bimbila sandstones

	Yabraso	**Bimbila**
1. Grain size	Medium-Fine	Medium-fine
2. Sorting	Moderately sorted	Moderately-well sorted
3. Roundness	Subangular to angular showing sharp terminations and straight edges	Well-rounded to subrounded
4. Packing	Packed	Loosely packed
5. Structures	Intergranular pores, quartz overgrowth	quartz overgrowth
6. Cement	Fe cement	Fe cement
7. Classification	Sub-arkose to quartz arenites	Sub-arkose to quartz arenites

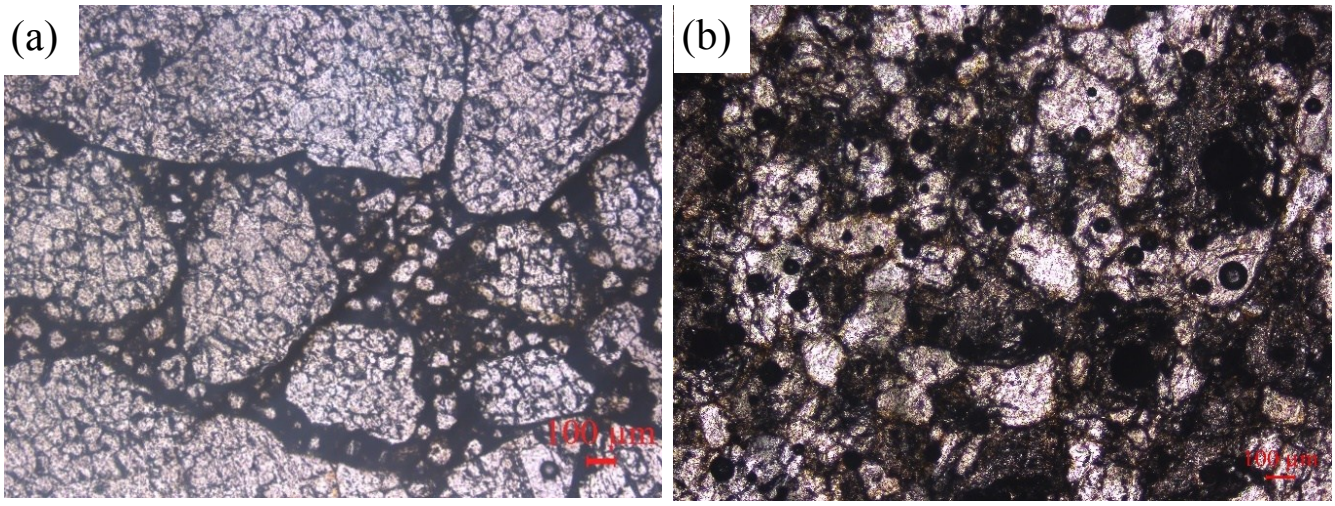

Figure 17 Photomicrographs of (a) loosely packed and moderately to poorly sorted Yabraso Sandstone grains (ppl, x5) and (b) well sorted Bimbila sandstone grains (ppl, x5)

63.41 mD. Though the porosity difference is not much, the clear difference in permeability values shows that the Bimbila Sandstone has better fluid transmission capabilities than the Yabraso as the permeability indicates a more ease of flow in the rock further confirmed by the photomicrograph of the stained Bimbila Sandstone (see Figure 14). Studies conducted on both the Bimbila and Yabraso Sandstones show that they have parameters making them suitable for fluid holding and transmission based on the porosity and permeability values recorded. However, the Bimbila Sandstones proved to have better porosity and permeability through grain sizes, shape, sorting and arrangement, grain coating, petrographic staining and petrophysical interpretations.

Conclusions

Petrophysical and petrographic techniques were used in this study to analyze the fluid holding and transmission capabilities of the Yabraso and Bimbila sandstone core samples. The voids (porosity), and their connectivity (permeability) were determined. Furthermore, the mineralogy was also studied and reported. The porosities of ten (10) Bimbila and twelve (12) Yabraso sandstone samples were determined in the laboratory using helium porosimetry. The porosity values where then used to estimate permeability using the Timur and Morris-Biggs correlations.

The Bimbila Sandstones showed better fluid holding and transmission capabilities with an average porosity of 14 % and permeability of 131.80 mD. Porosity range for Bimbila sandstone samples showed that 4 samples fall within the range of poor porosity (5-10 %), 2 samples have good porosity (10-20 %) and 4 samples have very good porosities (20-30 %). Permeability range of the Bimbila Sandstone samples for Timur correlation showed that 2 samples have poor permeability (Below 1 mD), 2 samples have fair permeability (1-10 mD), 1 sample has moderate permeability (10-50 mD), 2 samples have good permeability (50-250 mD) and 3 samples have very good permeability (above 250 mD) and for Morris-Biggs, 4 samples have poor permeability (Below 1 mD), 1 sample has fair permeability (1-10 mD), 1 sample has moderate permeability (10-50 mD), 3 samples have good permeability (50-250 mD) and 1 sample has very good permeability (above 250 mD). This is induced by less compaction, which is supported by framework-stable quartz cements, resulting in a sizable, interconnected pore structure with high permeability.

The Yabraso sandstones on the other hand showed that for Timur correlation, 3 samples have fair permeability (1-10 mD), 6 samples have moderate permeability (10-50 mD), 1 sample has good permeability (50-250 mD) and 2 samples have very good permeability (above 250 mD) and for Morris-Biggs correlation, 3 samples have poor permeability (Below 1 mD), 4 samples have fair permeability (1-10 mD), 2 samples have moderate permeability (10-50 mD), 2 samples have good permeability (50-250 mD) and 1 sample has very good permeability (above 250 mD). And the porosity range for the Yabraso showed that 3 samples fall within the range of poor porosity (5-10 %), 7 samples have good porosity (10-20 %) and only 2 samples have very good porosities (20-30 %). These differences between the Yabraso and Bimbila porosities and permeabilities are considered to be the result of diagenesis, which is influenced by the combined effect of the depositional environment and composition.

The position of the Yabraso and Bimbila Sandstones in the project area as plotted on the geological map show that there is a proximity relationship between these sandstones and the limestones (source rocks) hence forming a conducive system such that if hydrocarbons are produced by the possible source rocks (limestones), they can be housed by the sandstones showing good porosities and permeabilities.

In future research works on the basin, statistical constraining of horizontal and vertical permeability in the sandstones may be improved with more research using a larger data set. Also, more detailed field work like pitting and trenching should be conducted in the project area to deduce the thickness of the rocks.

Acknowledgement

This work was funded by the Ghana National Petroleum Corporation (GNPC) Petroleum Engineering Chair under the auspices of the Department of Petroleum Engineering of the Kwame Nkrumah University of Science and Technology, Kumasi, Ghana. The Grant Number is PE-001-201,901-0102.

Conflict of Interest Declarations

The authors declare no competing interests.

References

Abu, M., Adeleye, M. A., Ehinola, O. A., and Asiedu, D. K. (2021). The hydrocarbon prospectivity of the Mesoproterozoic–Paleozoic intracratonic Voltaian Basin, West African Craton, Ghana. Journal of Petroleum Exploration and Production, 11(2), pp. 617-625. https://doi.org/10.1007/s13202-020-01036-7

Adenutsi, C. D., Li, Z., Xu, Z., Hama, A. E., Sun, L., and Lai, F. (2019). Effect of silica nanofluid on nanoscopic pore

structure of low-permeability petroleum reservoir by nitrogen adsorption technique: a case study. Arabian Journal for Science and Engineering, pp. 44, 6167-6178. https://doi.org/10.1007/s13369-018-03708-3

Affaton, P., Rahaman, M. A., Trompette, R., and Sougy, J. (1991). The Dahomeyide Orogen: tectonothermal evolution and relationships with the Volta Basin. In The West African orogens and circum-Atlantic correlatives (pp. 107-122). Springer. https://doi.org/10.1007/978-3-642-84153-8_6

Affaton, P., Sougy, J., and Trompette, R. (1980). The tectonostratigraphic relationships between the Upper Precambrian and Lower Paleozoic Volta Basin and the Pan-African Dahomeyide orogenic belt (West Africa). American Journal Sciences, 280, pp. 224–248.

Ahmed, T. (2018). Reservoir engineering handbook. Gulf professional publishing pp.43.

Ajdukiewicz, J., Nicholson, P., and Esch, W. (2010). Prediction of deep reservoir quality using early diagenetic process models in the Jurassic Norphlet Formation, Gulf of Mexico. AAPG Bulletin, 94(8), pp. 1189-1227. https://doi.org/10.1306/04211009152

Anani, C. (1999). Sandstone petrology and provenance of the Neoproterozoic Voltaian Group in the southeastern Voltaian Basin, Ghana. Sedimentary Geology, 128(1-2), pp. 83-98. https://doi.org/10.1016/S0037-0738(99)00063-9

Becker, I., Wüstefeld, P., Koehrer, B., Felder, M., and Hilgers, C. (2017). Porosity and permeability variations in a tight gas sandstone reservoir analogue, Westphalian D, Lower Saxony Basin, NW Germany: influence of depositional setting and diagenesis. Journal of petroleum geology, 40 (4), pp. 363-389. https://doi.org/10.1111/jpg.12685

Boamah, K. (2017). Minerogeny of the Pan-African Volta Basin of Ghana. Doctoral dissertation, Technische Universität Bergakademie Freiberg pp. 1765. http://nbn-resolving.de/urn:nbn:de:bsz:105-qucosa-223299

Bozhko, N. (2008). Stratigraphy of the Voltaian basin on evidences derived from borehole loggins. The Voltaian Basin, Ghana Workshop and Excursion, pp. 10–17.

Bunaciu, A. A., UdriŞTioiu, E. G., and Aboul-Enein, H. Y. (2015). X-ray diffraction: instrumentation and applications. Critical reviews in analytical chemistry, 45(4), pp. 289-299. https://doi.org/10.1080/10408347.2014.949616

Busch, B. (2020). Pilot study on provenance and depositional controls on clay mineral coatings in active fluvio-eolian systems, western USA. Sedimentary Geology, pp. 406, 105721. https://doi.org/10.1016/j.sedgeo.2020.105721

Chudasama, B., Porwal, A., Kreuzer, O. P., and Butera, K. (2016). Geology, geodynamics and orogenic gold prospectivity modelling of the Paleoproterozoic Kumasi Basin, Ghana, West Africa. Ore Geology Reviews, 78, pp. 692-711. https://doi.org/10.1016/j.oregeorev.2015.08.012

Dayanım, J., Tablosunun, İ., and Kütle, K. (2017). The geological strength index chart assesment for rock mass permeability.

Dos Anjos, S. M., De Ros, L. F., de Souza, R. S., de Assis Silva, C. M., and Sombra, C. L. (2000). Depositional and diagenetic controls on the reservoir quality of Lower Cretaceous Pendencia sandstones, Potiguar rift basin, Brazil. AAPG Bulletin, 84(11), pp. 1719-1742. https://doi.org/10.1306/8626C375-173B-11D7-8645000102C1865D

Eisenlohr, B., and Hirdes, W. (1992). The structural development of the early Proterozoic Birimian and Tarkwaian rocks of southwest Ghana, West Africa. Journal of African Earth Sciences (and the Middle East), 14(3), pp. 313-325. https://doi.org/10.1016/0899-5362(92)90035-B

Folk, R. L. (1974). Petrology of sedimentary rocks: Austin. Texas, Hemphill, 182.

Grier, S., and Marschall, D. (1992). Reservoir quality: Part 6. Geological methods.

Griffiths, J., Worden, R. H., Wooldridge, L. J., Utley, J. E., and Duller, R. A. (2018). Detrital clay coats, clay minerals, and pyrite: a modern shallow-core analogue for ancient and deeply buried estuarine sandstones. Journal of Sedimentary Research, 88(10), pp. 1205-1237. https://doi.org/10.2110/jsr.2018.56

Guo, B., Sun, K., and Ghalambor, A. (2014). Well productivity handbook, pp. 32. Elsevier.

Heap, M. J., Kushnir, A. R., Gilg, H. A., Wadsworth, F. B., Reuschlé, T., and Baud, P. (2017). Microstructural and petrophysical properties of the Permo-Triassic sandstones (Buntsandstein) from the Soultz-sous-Forêts geothermal site (France). Geothermal Energy, 5(1), pp. 1-37. https://doi.org/10.1186/s40517-017-0085-9

Kesse, G. (1984). The occurrence of gold in Ghana. Gold'82: the geology, geochemistry and genesis of gold deposits symposium.

Koffi, Y. H., Wenmenga, U., and Djro, S. C. (2016). Tarkwaian deposits of the Birimian belt of Houndé: petrological, structural and geochemical study (Burkina-Faso, West Africa). International Journal of Geosciences, 7(05), pp. 685. http://dx.doi.org/10.4236/ijg.2016.75053

Legler, B., Schneider, J., Gebhardt, U., Merten, D., and Gaupp, R. (2011). Lake deposits of moderate salinity as sensitive indicators of lake level fluctuations: example from the Upper Rotliegend saline lake (Middle–Late Permian, Northeast Germany). Sedimentary Geology, 234(1-4), pp. 56-69. https://doi.org/10.1016/j.sedgeo.2010.11.006

Leube, A., Hirdes, W., Mauer, R., and Kesse, G. O. (1990). The early Proterozoic Birimian Supergroup of Ghana and some aspects of its associated gold mineralization. Precambrian research, 46(1-2), pp. 139-165. https://doi.org/10.1016/0301-9268(90)90070-7

Magoon, L. B. (2004). Petroleum system: Nature's distribution system for oil and gas. Encyclopedia of energy, 4, pp. 823-836.

McKinley, J. M., Atkinson, P. M., Lloyd, C. D., Ruffell, A. H., and Worden, R. (2011). How porosity and permeability vary spatially with grain size, sorting, cement volume, and mineral dissolution in fluvial Triassic sandstones: the value of geostatistics and local regression. Journal of Sedimentary Research, 81(12), pp. 844-858. https://doi.org/10.2110/jsr.2011.71

Milési, J., Ledru, P., Ankrah, P., Johan, V., Marcoux, E., and Vinchon, C. (1991). The metallogenic relationship between Birimian and Tarkwaian gold deposits in Ghana. Mineralium Deposita, 26(3), pp. 228-238. https://doi.org/10.1007/BF00209263

Monsees, A. C., Busch, B., and Hilgers, C. (2021). Compaction control on diagenesis and reservoir quality development in red bed sandstones: a case study of Permian Rotliegend sandstones. International Journal of Earth Sciences, 110(5), pp. 1683-1711. https://doi.org/10.1007/s00531-021-02036-6

Morad, S., Al-Ramadan, K., Ketzer, J. M., and De Ros, L. (2010). The impact of diagenesis on the heterogeneity of sandstone reservoirs: A review of the role of depositional facies and sequence stratigraphy. AAPG Bulletin, 94(8), pp. 1267-1309.

Quaye, J. A., Jiang, Z., Liu, C., Adenutsi, C. D., Adjei, S., Sarkodie, K., Sokama-Neuyam, Y. A., Lemdjou, Y. B., and Uahengo, C.-I. (2023). Understanding the role of bioturbation in modifying petrophysical properties: a case from well L5 of the third-member Paleocene Funing Formation (E1f3), Gaoyou Sag, Subei Basin, China. Arabian Journal of Geosciences, 16(7), pp. 407. https://doi.org/10.1007/s12517-023-11506-x

Quaye, J. A., Jiang, Z., Liu, C., Adenutsi, C. D., and Boateng, C. D. (2022). Biogenically modified reservoir rock quality: A case from the lowermost member Paleocene Funing Formation, Gaoyou Depression, Subei Basin, China. Journal of Petroleum Science and Engineering, 219, pp. 111126. https://doi.org/10.1016/j.petrol.2022.111126

Reineck, H.-E., and Singh, I. B. (2012). Depositional sedimentary environments: with reference to terrigenous clastics. Springer Science & Business Media.

Rossi, C., Kälin, O., Arribas, J., and Tortosa, A. (2002). Diagenesis, provenance and reservoir quality of Triassic TAGI sandstones from Ourhoud field, Berkine (Ghadames) Basin, Algeria. Marine and Petroleum Geology, 19(2), pp. 117-142. https://doi.org/10.1016/S0264-8172(02)00004-1

Satter, A., and Iqbal, G. M. (2015). Reservoir engineering: the fundamentals, simulation, and management of conventional and unconventional recoveries. Gulf Professional Publishing.

Schnurrenberger, D., Russell, J., and Kerry, K. (2003). Classification of lacustrine sediments based on sedimentary components. Journal of Paleolimnology, 29(2), pp. 141-154. https://doi.org/10.1023/A:1023270324800

Smith, A. J., Henry, G., and Frost-Killian, S. (2016). A review of the Birimian Supergroup-and Tarkwaian Group-hosted gold deposits of Ghana. Episodes, 39(2), pp. 177-197. https://doi.org/10.18814/epiiugs/2016/v39i2/95775

Sun, L., Hao, X., Dou, H., Adenutsi, C. D., and Liu, W. (2022). A novel model for predicting tight sandstone reservoir permeability. International Journal of Oil, Gas and Coal Technology, 29(1), pp. 75-90. https://doi.org/10.1504/IJOGCT.2022.119345

Terry, R. D., and Chilingar, G. V. (1955). Summary of" Concerning some additional aids in studying sedimentary formations," by MS Shvetsov. Journal of Sedimentary Research, 25(3), pp. 229-234. https://doi.org/10.1306/74D70466-2B21-11D7-8648000102C1865D

Tiab, D., and Donaldson, E. C. (2015). Petrophysics: theory and practice of measuring reservoir rock and fluid transport properties. Gulf professional publishing.

Timur, A. (1968). An investigation of permeability, porosity, and residual water saturation relation-ships for sandstone reservoir.

Toro, B. L., Li, Z., Adenutsi, C. D., and Abdullahi, S. M. (2018). Pore structure characterization of a low permeability reservoir using nuclear magnetic resonance, nitrogen adsorption and mercury intrusion capillary pressure. Petroleum & Coal, 60(2), pp. 23-25.

Walker, T., and Honea, R. (1969). Iron content of modern deposits in the Sonoran Desert: a contribution to the origin of red beds. Geological Society of America Bulletin, 80(3), pp. 535-544. https://doi.org/10.1130/0016-7606(1969)80[535:ICOMDI]2.0.CO;2

Worden, R., Mayall, M., and Evans, I. (2000). The effect of ductile-lithic sand grains and quartz cement on porosity and permeability in Oligocene and lower Miocene clastics, South China Sea: Prediction of reservoir quality. AAPG Bulletin, 84(3), pp. 345-359. https://doi.org/10.1306/C9EBCDE7-1735-11D7-8645000102C1865D

Yu, Z., Wang, Z., and Adenutsi, C. D. (2023). Genesis of authigenic clay minerals and their impacts on reservoir quality in tight conglomerate reservoirs of the Triassic Baikouquan formation in the Mahu Sag, Junggar Basin, Western China. Marine and Petroleum Geology, 148, pp. 106041. https://doi.org/10.1016/j.marpetgeo.2022.106041

Yuan, G., Cao, Y., Gluyas, J., Li, X., Xi, K., Wang, Y., Jia, Z., Sun, P., and Oxtoby, N. H. (2015). Feldspar dissolution, authigenic clays, and quartz cements in open and closed sandstone geochemical systems during diagenesis: Typical examples from two sags in Bohai Bay Basin, East China. AAPG Bulletin, 99(11), pp. 2121-2154. https://doi.org/10.1306/07101514004

Zhang, P., Lee, Y. I., and Zhang, J. (2019). A review of high-resolution X-ray computed tomography applied to petroleum geology and a case study. Micron, 124, pp. 102702. https://doi.org/10.1016/j.micron.2019.102702

Zobah, T. N., Adenutsi, C. D., Amedjoe, G. C., Wilson, M. C., Boateng, C. D., Quaye, J. A., Erzuah, S., Wang, L., Zhao, G., and Karimaie, H. (2022). A review on the provenance of the Voltaian Basin, Ghana: implications for hydrocarbon prospectivity. Scientific African, pp. 1429. https://doi.org/10.1016/j.sciaf.2022.e01429